Journal pre-proof

DOI: 10.1016/j.cell.2020.04.004

Inhibition of SARS-CoV-2 infections in engineered human tissues using clinical-grade soluble human ACE2

Vanessa Monteil[1], Hyesoo Kwon[2], Patricia Prado[3], Astrid Hagelkrüys[4], Reiner A. Wimmer[4], Martin Stahl[5], Alexandra Leopoldi[4], Elena Garreta[3], Carmen Hurtado del Pozo[3], Felipe Prosper[6], J.P. Romero[6], Gerald Wirnsberger[7], Haibo Zhang[8], Arthur S. Slutsky[8], Ryan Conder[5], Nuria Montserrat[3,9,10,*], Ali Mirazimi[1, 2,*], Josef M. Penninger[4,11,12*]

[1] Karolinska Institute and Karolinska University Hospital, Department of laboratory medicine, Unit of Clinical Microbiology, 17177, Stockholm, Sweden

[2] National Veterinary Institute, 751 89, Uppsala, Sweden

[3] Pluripotency for Organ Regeneration, Institute for Bioengineering of Catalonia (IBEC), The Barcelona Institute of Technology (BIST), 08028 Barcelona, Spain

[4] Institute of Molecular Biotechnology of the Austrian Academy of Sciences, Dr. Bohr-Gasse 3, 1030 Vienna, Austria.

[5] STEMCELL Technologies Inc., Vancouver, V6A 1B6, British Columbia, Canada

[6] Cell Therapy Program, Center for Applied Medical Research (CIMA), University of Navarra, 31008 Pamplona, Spain

[7] Apeiron Biologics, Campus Vienna Biocenter 5, 1030 Vienna, Austria.

[8] Keenan Research Centre for Biomedical Science at Li Ka Shing Knowledge Institute of St. Michael Hospital, University of Toronto, Toronto, M5B 1W8, Ontario, Canada

[9] Catalan Institution for Research and Advanced Studies (ICREA), 08010 Barcelona, Spain

[10] Centro de Investigación Biomédica en Red en Bioingeniería, Biomateriales y Nanomedicina, 28029 Madrid, Spain

[11] Department of Medical Genetics, Life Science Institute, University of British Columbia, Vancouver, V6T 1Z3, British Columbia, Canada.

[12] Lead Contact

Corresponding authors: Josef M Penninger (josef.penninger@ubc.ca), Ali Mirazimi (ali.mirazimi@sva.se), and Nuria Montserrat (nmontserrat@ibecbarcelona.eu)

Summary

We have previously provided the first genetic evidence that Angiotensin converting enzyme 2 (ACE2) is the critical receptor for SARS-CoV and that ACE2 protects the lung from injury, providing a molecular explanation for the severe lung failure and death due to SARS-CoV infections. ACE2 has now also been identified as a key receptor for SARS-CoV-2 infections and it has been proposed that inhibiting this interaction might be used in treating patients with COVID-19. However, it is not known whether human recombinant soluble ACE2 (hrsACE2) blocks growth of SARS-CoV-2. Here we show that clinical grade hrsACE2 reduced SARS-CoV-2 recovery from Vero cells by a factor of 1,000-5,000. An equivalent mouse rsACE2 had no effect. We also show that SARS-CoV-2 can directly infect engineered human blood vessel organoids and human kidney organoids, which can be inhibited by hrsACE2. These data demonstrate that hrsACE2 can significantly block early stages of SARS-CoV-2 infections.

Introduction

Outbreaks of emerging infectious diseases continue to challenge human health. The reported incidence of emerging and re-emerging zoonotic disease is increasing in many parts of the world. The Severe Acute Respiratory Syndrome Coronavirus (SARS-CoV) first emerged 17 years ago (Drosten et al., 2003). In December of 2019, a novel coronavirus (SARS-CoV-2) crossed species barriers to infect humans (Gorbalenya et al., 2020) and was effectively transmitted from person to person, leading to a pneumonia outbreak first reported in Wuhan, China (Guan et al., 2020; Jiang et al., 2020; Zhou et al., 2020b). This virus causes coronavirus disease-19 (COVID-19) with influenza like symptoms ranging from mild disease to severe lung injury and multi-organ failure, eventually leading to death, especially in older patients with other co-morbidities. The WHO has declared that COVID-19 is a public health emergency of pandemic proportions (https://www.who.int/). The SARS-CoV-2 pandemic is not only an enormous burden to public health but has already markedly affected civil societies and the global economy.

SARS-CoV-2 shares multiple similarities with SARS-CoV (Andersen et al., 2020; Lu et al., 2020; Zhu et al., 2020). Phylogenetic analysis of SARS-CoV-2 demonstrated that this virus belongs to lineage B of the betacoronavirus genus (Chan et al., 2020; Letko et al., 2020). The receptor binding domain (RBD) of SARS-CoV-2 is similar to the SARS-CoV RBD, suggesting a possible common host cell receptor. ACE2 was identified as the functional SARS-CoV receptor *in vitro* and, by our group, *in vivo* (Imai et al., 2005; Kuba et al., 2005). Overexpression of human ACE2 enhanced disease severity in mice infected with SARS-CoV, demonstrating that ACE2-dependent viral entry into cells is a critical step (Yang et al., 2007). We reported that injecting SARS-CoV spike into mice decreased ACE2 expression levels, thereby worsening lung injury (Imai et al., 2005; Kuba et al., 2005). Thus, ACE2 serves both as the entry receptor of SARS-CoV and to protect the lung from injury (Zhang et al., 2020b).

Three recent cryo-EM studies demonstrated that SARS-CoV-2 spike protein directly binds to ACE2 and that the SARS-CoV-2 spike protein recognizes human ACE2 with even higher binding affinity than Spike from SARS-CoV (Walls et al., 2020; Wan et al., 2020; Wrapp et al., 2020). Recently, it has been demonstrated in cell culture that soluble ACE2 fused to Ig (Wrapp et al., 2020) or a nonspecific protease inhibitor called camostat mesylate (Hoffmann et al., 2020), can inhibit infections with a Pseudovirus bearing the S protein of SARS-CoV-2. High doses (100μg/ml) of camostat mesylate were also shown to partially reduce SARS-CoV-2 growth, as expected from previous studies with other viruses (Hoffmann et al., 2020).

In a normal adult human lung, ACE2 is expressed primarily in alveolar epithelial type II cells, which can serve as a viral reservoir (Zhao et al., 2020). These cells produce surfactant which reduces surface tension, thus preventing alveoli from collapsing, and hence are critical to the gas exchange function of the lung (Dobbs, 1989). Injury to these cells could explain the severe lung injury observed in COVID-19 patients. We and others have also shown that ACE2 is expressed in multiple extrapulmonary tissues including heart, kidneys, blood vessels, and intestine (Crackower et al., 2002; Danilczyk and Penninger, 2006; Ding et al., 2004; Gu et al., 2005; Hamming et al., 2004; Zhang et al., 2020b). The ACE2 tissue distribution in these organs may explain the multi-organ dysfunction observed in patients (Guan et al., 2020; Huang et al., 2020). Here, we report that clinical-grade human recombinant soluble ACE2 (hrsACE2), which has already been tested in phase 1 and phase 2 clinical trials (Haschke et al., 2013, Khan et al., 2017), can reduce viral growth in Vero E6 cells by a factor of 1,000-5,000. Moreover, we show that human blood vessel organoids and kidney organoids can be readily infected, which can be significantly inhibited by hrsACE2 at the early stage of infection.

Results

Isolation of a SARS-CoV-2

To study potential therapeutic interventions for COVID-19, in early February 2020 we isolated the SARS-CoV-2 from a nasopharyngeal sample of a patient in Sweden with confirmed COVID-19. After successful culture on Vero E6 cells, the isolated virus was sequenced by Next-Generation Sequencing (Genbank accession number MT093571). Electron microscopy showed the prototypic coronal shape of viral particles of our SARS-CoV-2 isolate (Figure 1A). Phylogenetic analysis showed the virus belongs to the clad A3 (Figure 1B).

hrsACE-2 can inhibit SARS-CoV-2 infection in a dose dependent manner

hrsACE2 has already undergone clinical phase 1 and phase 2 testing (Khan et al., 2017) and is being considered for treatment of COVID-19 (Zhang et al., 2020b). Since ACE2 is the SARS-CoV-2 receptor, we wanted to provide direct evidence that clinical-grade hrsACE2 can indeed interfere with SARS-CoV-2 infections. To this end, we infected Vero-E6 cells (cells used for SARS-CoV-2 isolation) with different numbers of SARS-CoV-2: 10^3 plaque forming units (PFUs; MOI 0.02), 10^5 PFUs (MOI 2) and 10^6 PFUs (MOI 20). Viral RNA as a marker for replication was purified from cells and assayed by qRT-PCR (Figure 2A). Infection of cells in the presence of hrsACE2 during 1 hr, followed by washing and incubation without hrsACE2 significantly inhibited SARS-CoV-2 infections of Vero-E6 15 hours post infection (Figure 2A).

These data demonstrate that hrsACE2 inhibits the attachment of the virus to the cells. Importantly, as expected from a neutralizing agent, this inhibition was dependent on the initial quantity of the virus in the inoculum and the dose of hrsACE2 (Figure 2A), establishing dose-dependency. In contrast to hsrACE-2, the equivalent mouse recombinant soluble ACE2 (mrsACE2), produced in the same way as hrsACE2, did not inhibit the infection (Figure 2B). Finally, we performed experiments where cells were infected with SARS-CoV-2 in the presence of hrsACE2 or mrsACE2 for 15 hr, to capture any newly produced virus particles during the 15hr that could infect neighbouring cells. Again, we observed significantly reduced virus infections in the presence of hrsACE2 (Figure 2C), but not mrsACE2 (Figure 2D). Of note, addition of human or mouse rsACE2 was not toxic to the Vero-E6 cells, monitored for 15 hours (data not shown). These data show that hrsACE2 significantly reduces SARS-CoV-2 infections *in vitro*.

hrsACE-2 inhibits SARS-CoV-2 infections of human capillary organoids

A primary site of SARS-CoV-2 infection appears to be the lung, which may be a source for viral spread to other tissues such as the kidney and intestine, where virus has been found (stool and urine) (Ling et al., 2020; Young et al., 2020). Moreover, viremia is established during the course of the disease, although viral RNA in blood is only infrequently observed (Peng et al., 2020; Wang et al., 2020). However, the virus has a size of 80-100nm indicating that viremic SARS-CoV-2 must first infect blood vessels prior to local tissue infections. To test this hypothesis, we established human capillary organoids from induced pluripotent stem cells (iPSCs) (Figure 3A) and infected them with our SARS-CoV-2 isolate. Of note, these organoids closely resemble human capillaries with a lumen, $CD31^+$ endothelial lining, $PDGFR^+$ pericyte coverage, as well as formation of a basal membrane (Wimmer et al., 2019). The capillary organoids were analysed by qRT-PCR for the presence of viral RNA at day 3 and 6 after primary SARS-CoV-2 exposure. Importantly, following infection, we could detect viral RNA in the blood vessel organoids with viral RNA increasing from day 3 to day 6 post infection (Figure 3B), indicating active replication of SARS-CoV-2.

Supernatant of infected organoids collected at day 6 post-infection could efficiently infect Vero E6 cells (Figure 3C), showing that the infected capillary organoids produced progeny virus. Importantly, addition of hrsACE2 markedly reduced SARS-CoV-2 infections of the engineered human blood vessels (Figure 3D). Of note, addition of human or mouse rsACE2 was not toxic to human blood-vessels, monitored for 3 days (data not shown). These data show that human capillary organoids can be infected with SARS-CoV-2 and this infection can be significantly inhibited by hrsACE2.

hrsACE-2 can inhibit SARS-CoV-2 infections of human kidney organoids

We and others have previously shown that ACE2 is strongly expressed in kidney tubules (Danilczyk and Penninger, 2006). Moreover, it has been reported that SARS-CoV-2 can be found in the urine (Young et al., 2020). To test whether SARS-CoV2 can directly infect human tubular kidney cells, we generated kidney organoids from human embryonic stem cells into 3D suspension culture, adapting our own protocol (Garreta et al., 2019). Importantly, kidney differentiation organoids demonstrated prominent tubular-like structures as detected by Lotus Tetraglobus Lectin (LTL) as a marker of proximal tubular epithelial cells (Figure 4A). Tubular-like cells also expressed the solute carrier SCL3A1 (Figure S1A) together with SCL27A2 and SCL5A12. Furthermore, LTL positive (LTL^+) cell fractions from organoids expressed markers of proximal tubular identity (Figure S1B and S1C). Single cell profiling of kidney organoids showed the presence of cells expressing ACE2 in the proximal tubule and podocyte II cell clusters that express key marker genes of proximal tubular cells (SLC3A1, SLC27A2) and podocytes (PODXL, NPHS1, NPHS2), respectively (Figure S2). Thus, kidney organoids contain cell clusters that express ACE2 in a similar fashion to that observed in the native tissue (Lin et al. 2020).

Infections of kidney organoids were monitored 6 days after SARS-CoV-2 infection and assayed for the presence of viral RNA using q-RT-PCR. Progeny virus was determined as above using re-infections of Vero E6 cells. As expected from cells and tissues that express ACE2, SARS-CoV-2 replicated in kidney organoids (Figure 4B). Supernatant of infected kidney organoids collected at day 6 post-infection could efficiently infect Vero E6 cells (Figure 4C), showing that the engineered kidney organoids produced infectious progeny virus. Importantly, addition of hrsACE2 significantly reduced SARS-CoV-2 infections of the human kidney organoids in a dose dependent manner (Figure 4D). Of note, addition of human or mouse rsACE2 was not toxic to the kidney, monitored for 3 days (data not shown). These data indicate that besides blood vessels, engineered human kidney organoids can also be infected with SARS-CoV-2 and this infection can be inhibited by hrsACE2.

Discussion

ACE2 took centre stage in the COVID-19 outbreak as the key receptor for the spike glycoprotein of SARS-CoV-2, as demonstrated in multiple structural and biochemical interaction studies (Wrapp et al., 2020; Zhou et al., 2020b). Moreover, multiple drug development projects, including development of vaccines are focusing on the ACE2-SARS-CoV-2 Spike interactions. We initially identified mammalian ACE2 when we realized that flies carry two orthologues of ACE (Angiotensin-converting enzyme). Our first *ace2* mutant mice then demonstrated that ACE2 is a

negative regulator of the renin-angiotensin system (RAS) and genetically controls cardiovascular function and damage of multiple organs such as the lung, liver, and kidney (Clarke and Turner, 2012; Crackower et al., 2002). ACE2 catalytically removes the last amino acid of angiotensin II, thereby counterbalancing ACE and Ang II actions and generating "beneficial" downstream peptides such as Ang1-7. ACE2 also catalytically acts on other peptides such as in the Apelin/APJ system (Clarke and Turner, 2012).

Importantly, we reported that ACE2 protects from lung injury, based on its catalytic domain, and that ACE2 is the critical *in vivo* SARS-CoV spike glycoprotein receptor (Imai et al., 2005; Kuba et al., 2005). Initially two receptors had been identified for SARS-CoV in cell lines, namely ACE2 (Li et al., 2003) and the lectin L-SIGN (Jeffers et al., 2004). The severity of SARS could be partially explained by SARS-CoV Spike protein binding to ACE2 at a molecular interaction site that does not interfere with its catalytic activity (Li et al., 2005), which then leads to endocytosis of the virus and loss of ACE2 (Kuba et al. 2005), establishing a vicious circle of viral infection and local loss of lung injury protection. This led to the initiation of a drug development program – the development of soluble recombinant human ACE2, a drug that has undergone phase 1 testing in healthy volunteers and phase 2 testing in some patients with acute respiratory distress syndrome (ARDS) (Haschke et al., 2013; Khan et al., 2017; Treml et al., 2010). Our data now show that this clinical-grade human ACE2 molecule - but not mouse soluble ACE2 - can significantly inhibit SARS-CoV-2 infections and reduce viral load by a factor of 1,000-5,000. However, as observed in antibody neutralizing experiments of many viruses, the inhibition is not complete, though clearly dose-dependent. This may be due to the fact that there might be other co-receptors/auxiliary proteins or even other mechanisms by which viruses can enter cells, as had been initially proposed for SARS (Jeffers et al., 2004; Qi et al., 2020). Such a second receptor has been also suggested based on clinical data: SARS transmissibility was very low possibly due to the low level expression of ACE2 in the upper respiratory tract (Bertram et al., 2012; Hamming et al., 2004). Transmissibility of SARS-CoV-2 is much greater than that of SARS-CoV, suggesting that SARS-CoV-2 might use a co-receptor and/or other factors which allow infection of ACE2 expressing cells in the upper respiratory tract (Lukassen et al., 2020). Most importantly, our results demonstrate that hrsACE2 significantly blocks SARS-CoV-2 infections, providing a rationale that soluble ACE2 might not only protect from lung injury but also block the SARS-CoV-2 from entering target cells.

Pathology due to SARS, MERS, and now COVID-19 is not limited to the lung; damage can occur in multiple organs (Gu et al., 2005; Wu and McGoogan, 2020; Yeung et al., 2016). ACE2 is expressed in various tissues including the heart, kidney tubules, the luminal surface of the small

intestine, and blood vessels (Crackower et al., 2002; Danilczyk and Penninger, 2006; Ding et al., 2004; Gu et al., 2005; Hamming et al., 2004; Zhang et al., 2020b), suggesting that SARS-CoV-2 could also infect these tissues. We now show that blood vessels as well as kidney organoids can be readily be infected by SARS-CoV-2. SARS-CoV-2 must enter the blood stream to infect other tissues. However, the size of the infectious viral particles is about 80-100nm (Wrapp et al., 2020). Thus, unless there is already tissue damage, the virus must enter vascular endothelial cells to migrate into the organs. Our data in engineered human capillary organoids now suggest that SARS-CoV-2 could directly infect blood vessel cells. Infected blood vessel organoids also shed progeny viruses. Importantly, hrsACE2 markedly inhibited SARS-CoV-2 infections of the vascular organoids.

ACE2 is strongly expressed in kidney tubules, controlling a local RAS circuit (Clarke and Turner, 2012; Hashimoto et al., 2012). As an infection model, we therefore engineered human kidneys organoids from stem cells differentiated to contain tubular networks (Garreta et al., 2019). We now show that SARS-CoV-2 can infect such human kidney organoids, resulting in infectious viral progeny, inhibited by hrsACE2. Clinically, SARS-CoV-2 has been found in the urine (Peng et al., 2020) and many patients with COVID-19 present with cardiovascular and renal dysfunctions (Huang et al., 2020; Yang et al., 2020; Zhang et al., 2020a; Zhou et al., 2020a). Whether direct viral infection of the vasculature and kidneys directly contribute to the observed multi-organ damage in COVID-19 patients needs to be established. Given the fact that cardiac cells express high levels of ACE2, and heart alterations were the first phenotype observed in our *ace2* mutant mice (Crackower et al. 2002), it will be important to expand on our studies to heart and in particular lung organoids to better understand the multi-organ dysfunction in patients with COVID-19.

Our study has limitations. The design of our studies focused on the early stages of infection, demonstrating that hrsACE2 can block early entry of SARS-CoV-2 infections in host cells. As such, we cannot make any predictions with respect to the effect of hrsACE2 in later stages of the disease process. Secondly, we did not study lung organoids, and the lung is the major target organ for COVID-19. Finally, the RAS system represents a complex network of pathways which are influenced by external processes which are not simulated in our model systems. To address these issues, further studies are needed to illuminate the effect of hrsACE2 at later stages of infection *in vitro* and *in vivo*.

Acknowledgments

We thank all members of our laboratories for critical input and suggestions. J.M.P. is supported by the Canada 150 Research Chair program. This work was partially supported by the CIHR grants 440347, FDN143285 and OV3-170344. This work has received funding from the European Research Council (ERC) under the European Union's Horizon 2020 research and innovation Programme (StG-2014-640525_REGMAMKID to P.P., and N.M.). NM is also supported by the Spanish Ministry of Economy and Competitiveness/FEDER (SAF2017-89782-R), the Generalitat de Catalunya and CERCA Programme (2017 SGR 1306) and Asociación Española contra el Cáncer (LABAE16006). C.H.P.is supported by Marie Skłodowska-Curie Individual Fellowships (IF) grant agreement no. 796590. E.G is funded by the EFSD/Boehringer Ingelheim European Research Programme in Microvascular Complications of Diabetes. A. M. is supported by the Swedish research Council 2018-05766. F.P is funded by ISCIII, RD16/0011/0005 and CIBER CB16/12/00489 Cofinanced with FEDER Funds.

Author contributions

V.M. performed all of the experiments involving SARS-CoV-2, including isolation and helped with manuscript editing. J.P., N.M. and A.M. designed the project and wrote the manuscript. H.K. performed all the qRT-PCR for virus involved experiment. A.R., A.H. and R.A.W developed blood vessel organoids for infectious studies. E.G., P.P. and C.H.P. derived kidney organoids and tubular cells and performed subsequent analysis including: quantitive PCR, immunofluorescence and the preparation of kidney organoid samples for RNA sequencing. F.P. and P.R. performed RNA single cell analysis. G.W. developed and produced clinical-grade hrsACE2. M.S., H.Z., A.S.S and R.C. helped for manuscript editing and design of experiments.

Declaration of interests

J.M.P. declares a conflict-of-interest as a founder, supervisory board member, and shareholder of Apeiron Biologics. G. Wirnsberger is an employee of Apeiron Biologics. Apeiron holds a patent on the use of ACE2 for the treatment of lung, heart, or kidney injury and applied for a patent to treat COVID-19 with hrsACE2 and use organoids to test new drugs for SARS-CoV-2 infections. Ryan Conder and Martin Stahl are employees of STEMCELL Technologies Inc.. A. S. has been a consultant to Apeiron Biologics.

Main figure legends

Figure 1. **SARS-CoV-2 Sweden virus analyses.**

A) Electron microscopy image of a viral particle of the Swedish SARS-CoV-2 isolate. **B)** Phylogenetic tree mapping the Swedish SARS-CoV-2 to clade A3.

Figure 2. Human recombinant soluble ACE2 (hrsACE2) blocks SARS-CoV-2 infections.

A) Different concentrations of human recombinant ACE2 (hrsACE2) were mixed with SARS-CoV-2 for 30 minutes and then added to the culture medium of Vero-E6 cells. Cells were washed after 1 hour post-infection (h.p.i.) and incubated with fresh medium. Cell were recovered 15 hours post-infection and viral RNA was assayed by qRT-PCR. Data are represented as mean ± SD.** P<0.01; *** P<0.001. **B)** Murine recombinant soluble ACE2 (mrsACE2) did not significantly affect SARS-CoV-2 infections of Vero-E6 cells, highlighting the specificity of hrsACE2 in blocking SARS-CoV-2 entry. mrsACE2 was mixed with SARS-CoV-2 for 30 minutes and then added to the culture medium of Vero E6 cells. Cells were washed after 1 h.p.i and incubated with fresh medium. Cell were recovered 15 hours post-infection and viral RNA was assayed by qRT-PCR. Data are represented as mean ± SD **C)** Effect of hrsACE2 treatment on progeny virus. Vero E6 cells were infected with the indicated M.O.I. of SARS-CoV-2, (the inoculum was not removed). Cells were recovered 15 h.p.i. and viral RNA was assayed by qRT-PCR. Inhibition of the progeny virus by hsrACE2 resulted in significantly reduced virus infections Data are represented as mean ± SD (Student t test: *P<0.05; ** P<0.01). **D)** Murine recombinant soluble ACE2 (mrsACE2) did not significantly affect SARS-CoV-2 infections of Vero-E6 cells, highlighting the specificity of hsrACE2 in blocking SARS-CoV-2 entry. Vero-E6 cells were infected with the indicated M.O.I. of SARS-CoV-2 treated with murine recombinant soluble ACE2. Cells were harvested at 15 h.p.i and viral RNA was assayed by qRT-PCR.

Figure 3. SARS-CoV-2 infections of blood vessels organoids.

A) Representative images of vascular capillary organoids using light microscopy (magnifications x 10) (upper panels) and immunostaining of blood vessel organoids using anti-CD31 to detect endothelial cells and anti-PDGFRβ to detect pericytes. DAPI (blue) was used to visualize nuclei. Scale bars, 500μm and 50μm (inset). **B)** Recovery of viral RNA from blood vessel organoids at day 3 and 6 post-infection (dpi) with SARS-CoV-2, demonstrating that the virus can infect the vascular organoids. Data are represented as mean ± SD. **C)** Determination of progeny virus. Supernatants of SARS-CoV-2 infected blood vessel organoids were collected 6 dpi and then used to infect Vero E6 cells. After 48 hours, Vero E6 cells were washed and viral RNA assessed by qRT-PCR. The data show that infected blood vessel organoids can produce progeny SARS-CoV-2 viruses, depending on the initial level of infection. Data are represented as mean ± SD. **D)** Effect of hrsACE2 on SARS-CoV-2 infections of blood vessel organoids. Organoids were infected with

a mix of 10^6 infectious viral particles and hrsACE2 for 1 hour. 3 days post-infection, levels of viral RNA were assessed by qRT-PCR. hrsACE2 significantly decreased the level of SARS-CoV-2 infections in the vascular organoids Data are represented as mean ± SD (Student t test: ** P<0.01).

Figure 4. SARS-CoV-2 infections of human kidney organoids.

A) Representative images of a kidney organoid at day 20 of differentiation visualized using light microscopy (top left inset; Scale bar 100 μm) and confocal microscopy. Confocal microscopy images show tubular-like structures labelled with Lotus Tetraglobus Lectin (LTL, in green) and podocyte-like cells showing positive staining for Nephrin (in turquoise). Laminin (in red) was used as a basement membrane marker. DAPI labels nuclei. A magnified view of the boxed region shows a detail of tubular structures. Scale bars 250 and 100 μm, respectively. **B)** Recovery of viral RNA in the kidney organoids at day 6 post-infection (dpi) with SARS-CoV-2. Data are represented as mean ± SD. **C)** Determination of progeny virus. Supernatants of SARS-CoV-2 infected kidney organoids were collected 6 dpi and then used to infect Vero E6 cells. After 48 hours, Vero E6 cells were washed and viral RNA assessed by qRT-PCR. The data show that infected kidney organoids can produce progeny SARS-CoV-2 viruses, depending on the initial level of infection. Data are represented as mean ± SD. **D)** Effect of hrsACE2 on SARS-CoV-2 infections kidney organoids. Organoids were infected with a mix of 10^6 infectious viral particles and hrsACE2 for 1 hour. 3 days post-infection, levels of viral RNA were assessed by qRT-PCR. hrsACE2 significantly decreased the level of SARS-CoV-2 infections in the kidney organoids Data are represented as mean ± SD. (Student t test: * P<0.05).

Supplementary figure legends

Figure S1. Human kidney organoids as a surrogate of human proximal tubule cell culture model, related to Figure 4

A) Left image corresponds to a kidney organoid at day 20 of differentiation visualized using light microscopy. Scale bar 100 μm. Confocal microscopy images of tubular-like structures labelled with Lotus Tetraglobus Lectin (LTL, in green) and the proximal tubular cell marker SCL3A1 (in red). DAPI labels nuclei. A magnified view of the boxed region shows a detail of the tubular structures. Scale bars 250 and 50 μm, respectively. **B**) Expression changes of SLC3A1, SLC5A12 and SLC27A2 of bulk samples at day 20 of organoid differentiation. **C)** Left image corresponds to LTL^+ cells visualized using light microscopy. Scale bar 100 μm. Confocal microscopy images of LTL^+ cells labelled with Lotus Tetraglobus Lectin (LTL, in green) and the proximal tubular cell markers NaK ATPase (NaK, in red) and the solute carrier SGLT2 (in red). DAPI was used to visualize nuclei. Scale bars 100 μm.

Figure S2. Single cell RNA-seq analysis of kidney organoids reveals ACE2 expression in proximal tubule cells, related to figure 4

A) UMAP plot displaying the results after unbiased clustering. Subpopulations of renal endothelial-like, mesenchymal, proliferating, podocyte and tubule cells were identified. **B)** Expression of ACE2 projected in the UMAP reduction. **C)** Expression of different cellular markers: SLC3A1, SLC27A2 (Proximal Tubule); PODXL, NPHS1, NPHS2 (Podocyte); CLDN4, MAL (Loop of Henle) and CD93 (Renal Endothelial-like cells).

STAR METHOD

KEY RESOURCES TABLE

REAGENT or RESOURCE	SOURCE	IDENTIFIER
Antibodies		
Fluorescein labeled Lotus Tetragonolobus (LTL)	Vector Labs	FL-1321 RRID:AB_2336559
Anti-SLC3A1 polyclonal antibody	Merck	HPA038360-100U RRID:AB_2675975
Anti-SGLT2	Abcam	ab37296 RRID:AB_777895
Anti-LAMININ	Merck	L9393 RRID:AB_477163
Human Nephrin Affinity Purified Polyclonal Ab antibody	R&D Systems	AF4269 RRID:AB_2154851
Recombinant Anti-Sodium Potassium ATPase antibody	Abcam	ab209299 RRID:AB_1968790
Bacterial and Virus Strains		
SARS-CoV-2, GENBANK: MT093571	Isolated from patient	N/A
Biological Samples		
Chemicals, Peptides, and Recombinant Proteins		
CHIR99021	Merck	SML1046; CAS: 252917-06-9
Recombinant human FGF9	PeproTech	100-23
Heparin	Merck	H3149; CAS: 9041-08-1
Activin A	Vitro	338-AC-050
Paraformaldehyde solution 4% in PBS	Santa Cruz	sc-281692
1% Triton X-100	Merck	T8787
Glutaraldehyde	Sigma-Aldrich	G7776
srhACE2	Apeiron	N/A
Trizol	ThermoFisher	15596018
Recombinant Human VEGF165	Peprotech	100-20
Human FGF-2	Miltenyi Biotech	130-093-841
Critical Commercial Assays		
streptavidin/biotin blocking kit	Vector Labs	SP-2002
CellTiter-Glo® Luminescent cell viability assay	Promega	G7570
Direct-zol RNA MiniPrep kit	Zymo Reasearch	R2051
Chromium Single Cell 3' Library & Gel Bead Kit V**3**	10X Genomics (USA)	PN-1000075
NSQ 500/550 Hi Output KT v2.5 (75 CYS)	Illumina (San Diego, CA 92122 USA)	20024906
Sytox® blue dead cell stain	Thermofisher (Eugene, Oregon,USA)	S34857
Deposited Data		

Kidney Organoid scRNA-seq	This paper	GEO: GSE 147863
Experimental Models: Cell Lines		
ES[4] Human Embryonic Stem Cell line	The National Bank of Stem Cells (ISCIII,Madrid)	https://www.isciii.es/QueHacemos/Servicios/BIOBANCOS/BNLC/Lists/Lneas%20embrionarias/Attachments/6/Caracteristicas%20-%20Documento_Deposito_Lineas_v32_ES4_def.pdf
Vero E6 cells	ATCC	CRL-1586
Experimental Models: Organisms/Strains		
Oligonucleotides		
Primer: RPLP0 Forward: CCATTCTATCATCAACGGGTACAA Reverse: AGCAAGTGGGAAGGTGTAATCC	N/A	N/A
Primer: SLC3A1 Forward: CACCAATGCAGTGGGACAAT Reverse: CTGGGCTGAGTCTTTTGGAC	N/A	N/A
Primer: SLC27A2 Forward: TACTCTTGCCTTGCGGACTAA Reverse: CCGAAGCAGTTCACCGATATAC	N/A	N/A
Primer: SLC5A12 Forward: ACACGGTACAGACCTTCGTCA Reverse: GCTGCTCCCAGGTATTTGTC	N/A	N/A
Primer: SARS-CoV-2 E gene Forward: AGATTTGGACCTGCGAGCG Reverse: GAGCGGCTGTCTCCACAAGT	N/A	N/A
Primer: Human RNAse P Forward: ACAGGTACGTTAATAGTTAATAGCGT Reverse: ATATTGCAGCAGTACGCACACA	N/A	N/A
Recombinant DNA		
Human RNase P probe: FAM-TTCTGACCTGAAGGCTCTGCGCG-MGB	N/A	N/A
SARS-CoV-2 E gene probe: FAM-ACACTAGCCATCCTTACTGCGCTTCG-QSY	N/A	N/A
Software and Algorithms		
GraphPad Prism 8 (GraphPad)	(Motulsky and Brown, 2006)	http://www.graphpad.com
ImageJ	(Schneider et al., 2012)	https://imagej.net/ImageJ
FACSDiva software version 8.0.1 (BD Biosciences)	Becton, Dickinson and Company	https://www.bdbiosciences.com/en-us/instruments/research-instruments/research-software/flow-cytometry-acquisition/facsdiva-software
FlowJo software version 10	Becton, Dickinson and Company	https://www.flowjo.com/
Cell Ranger v3.0.1	10X Genomics	https://support.10xgenomics.com/single-cell-gene-expression/software/overview/welcome
R v3.5.1	R Core	https://cran.r-project.org/
Seurat v3.0.2	(Stuart et al., 2019)	https://satijalab.org/seurat/

Kidney Interactive Transcriptomics (KIT)	(Wu et al., 2018a)	http://humphreyslab.com/SingleCell/
Other		

RESOURCE AVAILABILITY

Lead Contact

Further information and requests for resources and reagents should be directed to and will be fulfilled by the Lead Contact, Joseph Penniger (josef.penninger@ubc.ca).

Materials Availability

All unique organoids generated in this study are available from the Lead Contact with a completed Materials Transfer Agreement.

Data and Code Availability

Raw sequencing data for the single cell kidney organoid reported in this paper were deposited in Gene Gene Expression Omnibus. (GEO) under the accession number GEO: GSE147863, GSM4447249.

Scripts reproducing the single cell kidney analysis are deposited in: https://github.com/jpromeror/SC_KidneyOrganoid_ACE2

EXPERIMENTAL MODEL AND SUBJECT DETAILS

Virus

SARS-CoV-2 was isolated on Vero-E6 cells, from a nasopharyngeal sample of a patient in Sweden. Virus was titered using a plaque assay as previously described (Becker et al., 2008) with fixation of cells 72 hours post infection. The SARS-CoV-2 isolate was sequenced by Next-Generation Sequencing (Genbank accession number MT093571). For electron microscopy, viral stocks were inactivated using 35% Glutaraldehyde.

Cells and human capillary organoids

Vero-E6 cells (ATCC) were grown in Dulbecco's Modified Eagle's Medium (DMEM, Thermofisher) supplemented with 1% Non-Essential Amino-Acid (Thermofisher), 10mM Hepes (Thermofisher) and 10% FBS at 37°C, 5% CO2. Blood vessels organoids were engineered from human iPS cells and immunostained as previously described (Wimmer et al., 2019a).

METHOD DETAILS

Preparation of soluble recombinant human and murine ACE2

Clinical-grade soluble recombinant human ACE2 (amino acids 1-740) was produced by Polymun Scientific (contract manufacturer) from CHO cells according to Good Manufacturing Practice guidelines and formulated as a physiologic aqueous solution. The equivalent domain of murine ACE2 was similarly overexpressed in CHO cells under serum free conditions and purified by sequentially performing a capture step on DEAE-Sepharose, ammonium sulfate precipitation, purification via a HIC-Phenyl Sepharose column, followed by purification via a Superdex 200 gel filtration column. The purity of the murine protein was determined via HPLC, concentrations were determined with 280nm photometric measurements.

Kidney organoid differentiation

Human embryonic stem cells were grown on vitronectin coated plates (1001-015, Life Technologies) and incubated with 0.5mM EDTA (Merck) at 37oC for 3 minutes for disaggregation. 100,000 cells/well were plated on a 24 multi-well plate coated with 5µl/ml vitronectin and further incubated with supplemented Essential 8 Basal medium at 37oC overnight. The day after (day 0), cells were treated for 3 subsequent days in Advanced RPMI 1640 basal medium (ThermoFisher) supplemented with 8µM CHIR (Merck) and 1% Penicillin-Streptomycin and 1% of GlutaMAX TM (ThermoFisher). The medium was changed every day. From day 3 to 4, media were changed to Advanced RPMI supplemented with 200ng/ml FGF9 (Peprotech), 1µg/ml heparin (Merck) and 10ng/ml activin A (Vitro). On day 4, cultures were rinsed twice with PBS, and resuspended in Advanced RPMI supplemented with 5µM CHIR, 200ng/ml FGF9 and 1µg/ml Heparin. Cellular suspensions were seeded in V-shape 96 multi-well plate at a final concentration of 100,000 cells/well and centrifugated at 2000 rpm for 3 minutes. The resulting spheroids were incubated during 1h at 37ºC. Culture media was replaced by Advanced RPMI supplemented with 200ng/ml FGF9 and 1µg/ml Heparin for 7 additional days, the media was changed every second day. From day 11 to 16, developing organoids were incubated only in the presence of Advanced RPMI, the media was every second day.

Phylogenetic analysis

To generate a phylogenetic tree, we created a genomic epidemiology map of different SARS-CoV-2 isolates using NextStrain tools (https://nextstrain.org/) (Hadfield et al., 2018). The sequences of the different isolates were obtained from GISAID (https://www.gisaid.org/) (Elbe and Buckland-Merrett, 2017). Screenshots is used under a CC-BY-4.0 license.

Treatments of Vero E6 cells with human rsACE2 and murine rsACE2

Vero E6 cells were seeded in 48-well plates (5.10^4 cells per well) (Sarstedt) in DMEM containing 10% FBS. 24 hours post-seeding, hrsACE2 or mrsACE2 were mixed with different concentration of virus (1:1) in a final volume of 100µl per well in DMEM (0% FBS) at 37°C. After 30 minutes, Vero-E6 were infected either with mixes containing hrsACE2/SARS-CoV-2 and mrsACE2/SARS-CoV-2 for 1 hour followed by washing or for 15 hours without washing, cells were washed 3 times with PBS and 500µl of new complete medium supplemented with hrsACE2 or mrsACE2 were added. 15 hours post-infection, supernatants were removed, cells were washed 3 times with PBS and then lysed using Trizol™ (Thermofisher) before analysis by qRT-PCR for viral RNA detection.

SARS-CoV-2 infections of kidney and blood vessel organoids

Kidney organoids were infected with 10^3 or 10^5 SARS-CoV-2 infectious particles in advanced RPMI medium (Thermofisher). Blood vessels organoids were infected with 10^2, 10^4, or 10^6 SARS-CoV-2 infectious particles in StemPro complete media containing 15% FBS (Gibco cat.10500064), 100ng/ml of VEGF-A (Peprotech cat. no. 100-20) and 100ng/ml of FGF-2 (Milteny Biotech cat. no. 130-093-841) as previously described (12) in a volume of 50µl per well of a 96-well ultra-low attachment plate for 1 hour. One hour post-infection, organoids were washed 3 times with PBS and kept in 100µl of corresponding medium for 3 to 6 days. On day 3 post-infection, organoids were washed 3 times with PBS before being lysed with Trizol™ (Thermofisher). At day 6 post-infection, supernatants were recovered and organoids washed 3 times with PBS before to lysis with Trizol™ (Thermofisher). Samples were then analysed for the presence of viral RNA by qRT-PCR. 100µl of each supernatant were used to infect Vero E6 in 48-well plate plates. Cells were recovered 48 hours post-infection, pooled (5 blood-vessels organoids/ condition, 3 kidney organoids/condition), and the level of infection was determined by viral RNA detection using qRT-PCR.

Treatment of organoids with hrsACE2

Different concentrations of hrsACE2 were mixed with 106 particles of SARS-CoV-2 for 30min at 37°C in a final volume of 50µl per well in STemPro 34 complete medium (blood-vessels) or advanced RPMI medium (Kidneys) as described above. Organoids were then infected with the mixes for 1 hour at 37°C, washed 3 times with PBS and 100µl per well of new medium was added. To detect intracellular viral RNA, organoids were washed 3 times with PBS, pooled (5 organoids/condition for blood-vessels; 3 organoids/condition for kidneys) and lysed using Trizol™ (Thermofisher) before analysis by qRT-PCR for viral RNA detection.

Cytotoxicity assay

To determine whether human or mouse rsACE2 are toxic to cells, 10^4 Vero E6 cells per well were seeded in a 96-well plate. 24h post-seeding, 25µl of different concentrations (25 – 200µg/ml of rsACE2 were added in triplicate and incubated for 15h. 15h post-treatment, cytotoxicity was determined using the CellTiter-Glo® Luminescent cell viability assay (Promega) following the following the manufacturer's protocol using 50µl of CellTiter-Glo® Reagent per well.

qRT-PCR

Samples were extracted using Direct-zol RNA MiniPrep kit (Zymo Research). qRT-PCR was performed using E-gene SARS-CoV-2 primers/probe following guidelines by the World Health Organization (https://www.who.int/docs/default-source/coronaviruse/wuhan-virus-assay-v1991527e5122341d99287a1b17c111902.pdf)

Forward primer: 5´-ACAGGTACGTTAATAGTTAATAGCGT-3'

Reverse primer: 5´-ATATTGCAGCAGTACGCACACA-3'

Probe: FAM-ACACTAGCCATCCTTACTGCGCTTCG-QSY

RNase P was used as an endogenous gene control to normalize the levels of intracellular viral RNA.

Forward primer: AGATTTGGACCTGCGAGCG

Reverse primer GAGCGGCTGTCTCCACAAGT

probe: FAM-TTCTGACCTGAAGGCTCTGCGCG-MGB

Primers used for tubular markers in kidney organoids are listed in Supplementary Table 1.

Single cell sequencing of kidney organoids

Kidney organoids were homogenized using 21G and 26 1/2G syringes and further dissociated using Accumax (07921, Stem Cell Technologies9 for 15 min at 37ºC followed by Trypsin-EDTA 0,25% (wt/vol) trypsin (25300-054, Life Technologies) for additional 15 min at 37ºC. The reaction was deactivated by adding 10% FBS. The solution was then passed through a 40 µm cell strainer and frozen in Advanced RPMI 1640 basal medium (ThermoFisher) in the presence of DMSO10%. Cells were thawed and centrifuged at 1,500 RPM for 5 minutes, stained with sytox blue (Thermofisher) and sorted by FACS to remove the nonviable cells, generating a single cell suspension with greater than 90% viability analyzed using the cellometer K2 (Nexcelom Biocience). Libraries were prepared using the Chromium Single Cell 3′ GEM, v3, (PN-1000075, 10X genomics) following the manufacturer´s instructions and sequenced with a NEXTseq500 (R1:28, R2: 55, i7:8) up to 30.000 reads per cell.

Histological analysis

Kidneys organoid and LTL+ cells were washed with PBS. Next samples were fixed with 4% paraformaldehyde (153799, Aname) for 20 min at room temperature. Specimens were washed twice with PBS and further blocked using Tris-buffered saline (TBS) with 6% donkey serum (S30, Millipore) and 1% Triton X-100 (T8787, Sigma) for 1h at room temperature. After three rinses with antibody dilution buffer, samples were treated for 4h at room temperature with fluorescent conjugated secondary antibodies (Alexa Fluor (A) Cy3- or A647-; 1:200). A previous blocking step with a streptavidin/biotin blocking kit (SP-2002, Vector Labs) was performed for biotinylated LTL (B-1325, Vector Labs) and Alexa Fluor 488-conjugated streptavidin (SA5488, VectorLabs) to detect LTL+ cells. Antibodies to NEPHRIN (R&D SYSTEMS 4269; 1:100) and LAMININ (Sigma L9393; 1:50), SGLT2 (Abcam AB37296; 1:100), NaKATPase (Abcam; AB209299; 1:200) and SLC3A1 (Sigma HPA038360; 1:50) were used overnight at 4°C diluted in antibody dilution buffer consisting of TBS with 6% donkey serum and 0.5% Triton X-100. Nuclei were detected using 4,6-diamidino-2-phenylindole (DAPI; 1:5000, D1306, Life Technologies) for 30min. For mounting, samples were immersed in Fluoromount-G (0100-01, Southern Biotech). Sample confocal images were acquired with an SP5 Leica microscope and LTL + were analysed using Image J.

Flow cytometry

For the isolation of LTL+ cells kidney organoids were stained with fluorescein-conjugated LTL (FL-1321, Vector Laboratories). Then specimens were dissociated to single cells using Accumax (07921, Stem Cell Technologies) for 15min followed by 0.25% (wt/vol) trypsin (25300–054, Life Technologies) for 15min at 37 °C. For LTL+ cells isolation FACSDiva software version 8.0.1 (BD Biosciences) was used in the FACS Aria Fusion instrument (BD Biosciences).

QUANTIFICATION AND STATISTICAL ANALYSIS

Kidney Organoid scRNA-seq Data Analysis

Libraries were pre-processed using Cell Ranger (3.0.1) from 10X Genomics. The computational analysis was performed using Seurat (3.0.2) (Stuart et al., 2019). Initial quality control parameters were defined based on the distributions of the number of detected genes per cell, the number of UMIs per cell and the % of UMIs assigned to mitochondrial genes. The selected thresholds were: 668 < UMIs per cell < 23101, 489 < Genes per cell < 5651 and % UMIs assigned to mitochondrial genes < 50. The dataset was subjected to normalization, identification of highly variable features and scaling using the SCTransform function of the Seurat package. Principal component analysis was performed, and 20 components were kept for further analysis. Clustering was performed by setting the resolution parameter to 0.4. Dimensional reduction was done using the RunUMAP

function of the Seurat R package. Cell markers were identified by using a Wilcoxon test. Genes with adjusted p.value < 0.5 were retained. Clusters were labelled by comparing the expression of the identified markers with publicly available databases (Wu et al., 2018b) located in KIT (Kidney Interactive Transcriptomics webpage (http://humphreyslab.com/SingleCell/).

Statistics.

Statistical analyses were conducted using GraphPad Prism 8 (GraphPad) and significance was determined by Students t-test.

References

Andersen, K.G., Rambaut, A., Lipkin, W.I., Holmes, E.C., and Garry, R.F. (2020). The proximal origin of SARS-CoV-2. Nature Medicine.

Bertram, S., Heurich, A., Lavender, H., Gierer, S., Danisch, S., Perin, P., Lucas, J.M., Nelson, P.S., Pohlmann, S., and Soilleux, E.J. (2012). Influenza and SARS-coronavirus activating proteases TMPRSS2 and HAT are expressed at multiple sites in human respiratory and gastrointestinal tracts. PLoS One *7*, e35876.

Chan, J.F., Kok, K.H., Zhu, Z., Chu, H., To, K.K., Yuan, S., and Yuen, K.Y. (2020). Genomic characterization of the 2019 novel human-pathogenic coronavirus isolated from a patient with atypical pneumonia after visiting Wuhan. Emerg Microbes Infect *9*, 221-236.

Clarke, N.E., and Turner, A.J. (2012). Angiotensin-converting enzyme 2: the first decade. Int J Hypertens *2012*, 307315.

Crackower, M.A., Sarao, R., Oudit, G.Y., Yagil, C., Kozieradzki, I., Scanga, S.E., Oliveira-dos-Santos, A.J., da Costa, J., Zhang, L., Pei, Y., *et al.* (2002). Angiotensin-converting enzyme 2 is an essential regulator of heart function. Nature *417*, 822-828.

Danilczyk, U., and Penninger, J.M. (2006). Angiotensin-converting enzyme II in the heart and the kidney. Circ Res *98*, 463-471.

Ding, Y., He, L., Zhang, Q., Huang, Z., Che, X., Hou, J., Wang, H., Shen, H., Qiu, L., Li, Z., *et al.* (2004). Organ distribution of severe acute respiratory syndrome (SARS) associated coronavirus (SARS-CoV) in SARS patients: implications for pathogenesis and virus transmission pathways. J Pathol *203*, 622-630.

Dobbs, L.G. (1989). Pulmonary surfactant. Annu Rev Med *40*, 431-446.

Drosten, C., Gunther, S., Preiser, W., van der Werf, S., Brodt, H.R., Becker, S., Rabenau, H., Panning, M., Kolesnikova, L., Fouchier, R.A., *et al.* (2003). Identification of a novel coronavirus in patients with severe acute respiratory syndrome. N Engl J Med *348*, 1967-1976.

Garreta, E., Prado, P., Tarantino, C., Oria, R., Fanlo, L., Marti, E., Zalvidea, D., Trepat, X., Roca-Cusachs, P., Gavalda-Navarro, A., *et al.* (2019). Fine tuning the extracellular environment accelerates the derivation of kidney organoids from human pluripotent stem cells. Nat Mater *18*, 397-405.

Gorbalenya, A.E., Baker, S.C., Baric, R.S., de Groot, R.J., Drosten, C., Gulyaeva, A.A., Haagmans, B.L., Lauber, C., Leontovich, A.M., Neuman, B.W., *et al.* (2020). The species Severe acute respiratory syndrome-related coronavirus: classifying 2019-nCoV and naming it SARS-CoV-2. Nature Microbiology *5*, 536-544.

Gu, J., Gong, E., Zhang, B., Zheng, J., Gao, Z., Zhong, Y., Zou, W., Zhan, J., Wang, S., Xie, Z., *et al.* (2005). Multiple organ infection and the pathogenesis of SARS. J Exp Med *202*, 415-424.

Guan, W.J., Ni, Z.Y., Hu, Y., Liang, W.H., Ou, C.Q., He, J.X., Liu, L., Shan, H., Lei, C.L., Hui, D.S.C., *et al.* (2020). Clinical Characteristics of Coronavirus Disease 2019 in China. N Engl J Med.

Hamming, I., Timens, W., Bulthuis, M.L., Lely, A.T., Navis, G., and van Goor, H. (2004). Tissue distribution of ACE2 protein, the functional receptor for SARS coronavirus. A first step in understanding SARS pathogenesis. J Pathol *203*, 631-637.

Haschke, M., Schuster, M., Poglitsch, M., Loibner, H., Salzberg, M., Bruggisser, M., Penninger, J., and Krahenbuhl, S. (2013). Pharmacokinetics and pharmacodynamics of recombinant human angiotensin-converting enzyme 2 in healthy human subjects. Clin Pharmacokinet *52*, 783-792.
Hashimoto, T., Perlot, T., Rehman, A., Trichereau, J., Ishiguro, H., Paolino, M., Sigl, V., Hanada, T., Hanada, R., Lipinski, S., *et al.* (2012). ACE2 links amino acid malnutrition to microbial ecology and intestinal inflammation. Nature *487*, 477-481.
Hoffmann, M., Kleine-Weber, H., Schroeder, S., Kruger, N., Herrler, T., Erichsen, S., Schiergens, T.S., Herrler, G., Wu, N.H., Nitsche, A., *et al.* (2020). SARS-CoV-2 Cell Entry Depends on ACE2 and TMPRSS2 and Is Blocked by a Clinically Proven Protease Inhibitor. Cell.
Huang, C., Wang, Y., Li, X., Ren, L., Zhao, J., Hu, Y., Zhang, L., Fan, G., Xu, J., Gu, X., *et al.* (2020). Clinical features of patients infected with 2019 novel coronavirus in Wuhan, China. Lancet *395*, 497-506.
Imai, Y., Kuba, K., Rao, S., Huan, Y., Guo, F., Guan, B., Yang, P., Sarao, R., Wada, T., Leong-Poi, H., *et al.* (2005). Angiotensin-converting enzyme 2 protects from severe acute lung failure. Nature *436*, 112-116.
Jeffers, S.A., Tusell, S.M., Gillim-Ross, L., Hemmila, E.M., Achenbach, J.E., Babcock, G.J., Thomas, W.D., Jr., Thackray, L.B., Young, M.D., Mason, R.J., *et al.* (2004). CD209L (L-SIGN) is a receptor for severe acute respiratory syndrome coronavirus. Proc Natl Acad Sci U S A *101*, 15748-15753.
Jiang, S., Du, L., and Shi, Z. (2020). An emerging coronavirus causing pneumonia outbreak in Wuhan, China: calling for developing therapeutic and prophylactic strategies. Emerg Microbes Infect *9*, 275-277.
Khan, A., Benthin, C., Zeno, B., Albertson, T.E., Boyd, J., Christie, J.D., Hall, R., Poirier, G., Ronco, J.J., Tidswell, M., *et al.* (2017). A pilot clinical trial of recombinant human angiotensin-converting enzyme 2 in acute respiratory distress syndrome. Crit Care *21*, 234.
Kuba, K., Imai, Y., Rao, S., Gao, H., Guo, F., Guan, B., Huan, Y., Yang, P., Zhang, Y., Deng, W., *et al.* (2005). A crucial role of angiotensin converting enzyme 2 (ACE2) in SARS coronavirus-induced lung injury. Nat Med *11*, 875-879.
Letko, M., Marzi, A., and Munster, V. (2020). Functional assessment of cell entry and receptor usage for SARS-CoV-2 and other lineage B betacoronaviruses. Nature Microbiology *5*, 562-569.
Li, F., Li, W., Farzan, M., and Harrison, S.C. (2005). Structure of SARS Coronavirus Spike Receptor-Binding Domain Complexed with Receptor. Science *309*, 1864-1868.
Li, W., Moore, M.J., Vasilieva, N., Sui, J., Wong, S.K., Berne, M.A., Somasundaran, M., Sullivan, J.L., Luzuriaga, K., Greenough, T.C., *et al.* (2003). Angiotensin-converting enzyme 2 is a functional receptor for the SARS coronavirus. Nature *426*, 450-454.
Ling, Y., Xu, S.B., Lin, Y.X., Tian, D., Zhu, Z.Q., Dai, F.H., Wu, F., Song, Z.G., Huang, W., Chen, J., *et al.* (2020). Persistence and clearance of viral RNA in 2019 novel coronavirus disease rehabilitation patients. Chin Med J (Engl).
Lu, R., Zhao, X., Li, J., Niu, P., Yang, B., Wu, H., Wang, W., Song, H., Huang, B., Zhu, N., *et al.* (2020). Genomic characterisation and epidemiology of 2019 novel coronavirus: implications for virus origins and receptor binding. Lancet *395*, 565-574.
Lukassen, S., Chua, R.L., Trefzer, T., Kahn, N.C., Schneider, M.A., Muley, T., Winter, H., Meister, M., Veith, C., Boots, A.W., *et al.* (2020). SARS-CoV-2 receptor ACE2 and TMPRSS2 are predominantly expressed in a transient secretory cell type in subsegmental bronchial branches. bioRxiv, 2020.2003.2013.991455.
Motulsky, H.J., and Brown, R.E. (2006). Detecting outliers when fitting data with nonlinear regression - a new method based on robust nonlinear regression and the false discovery rate. BMC Bioinformatics *7*, 123.
Peng, L., Liu, J., Xu, W., Luo, Q., Deng, K., Lin, B., and Gao, Z. (2020). 2019 Novel Coronavirus can be detected in urine, blood, anal swabs and oropharyngeal swabs samples. medRxiv, 2020.2002.2021.20026179.
Qi, F., Qian, S., Zhang, S., and Zhang, Z. (2020). Single cell RNA sequencing of 13 human tissues identify cell types and receptors of human coronaviruses. Biochemical and Biophysical Research Communications.
Schneider, C.A., Rasband, W.S., and Eliceiri, K.W. (2012). NIH Image to ImageJ: 25 years of image analysis. Nat Methods *9*, 671-675.

Stuart, T., Butler, A., Hoffman, P., Hafemeister, C., Papalexi, E., Mauck, W.M., 3rd, Hao, Y., Stoeckius, M., Smibert, P., and Satija, R. (2019). Comprehensive Integration of Single-Cell Data. Cell *177*, 1888-1902 e1821.
Treml, B., Neu, N., Kleinsasser, A., Gritsch, C., Finsterwalder, T., Geiger, R., Schuster, M., Janzek, E., Loibner, H., Penninger, J., *et al.* (2010). Recombinant angiotensin-converting enzyme 2 improves pulmonary blood flow and oxygenation in lipopolysaccharide-induced lung injury in piglets. Crit Care Med *38*, 596-601.
Walls, A.C., Park, Y.-J., Tortorici, M.A., Wall, A., McGuire, A.T., and Veesler, D. (2020). Structure, Function, and Antigenicity of the SARS-CoV-2 Spike Glycoprotein. Cell.
Wan, Y., Shang, J., Graham, R., Baric, R.S., and Li, F. (2020). Receptor recognition by novel coronavirus from Wuhan: An analysis based on decade-long structural studies of SARS. J Virol.
Wang, W., Xu, Y., Gao, R., Lu, R., Han, K., Wu, G., and Tan, W. (2020). Detection of SARS-CoV-2 in Different Types of Clinical Specimens. JAMA.
Wimmer, R.A., Leopoldi, A., Aichinger, M., Wick, N., Hantusch, B., Novatchkova, M., Taubenschmid, J., Hammerle, M., Esk, C., Bagley, J.A., *et al.* (2019). Human blood vessel organoids as a model of diabetic vasculopathy. Nature *565*, 505-510.
Wrapp, D., Wang, N., Corbett, K.S., Goldsmith, J.A., Hsieh, C.L., Abiona, O., Graham, B.S., and McLellan, J.S. (2020). Cryo-EM structure of the 2019-nCoV spike in the prefusion conformation. Science.
Wu, H., Malone, A.F., Donnelly, E.L., Kirita, Y., Uchimura, K., Ramakrishnan, S.M., Gaut, J.P., and Humphreys, B.D. (2018a). Single-Cell Transcriptomics of a Human Kidney Allograft Biopsy Specimen Defines a Diverse Inflammatory Response. J Am Soc Nephrol *29*, 2069-2080.
Wu, H., Uchimura, K., Donnelly, E.L., Kirita, Y., Morris, S.A., and Humphreys, B.D. (2018b). Comparative Analysis and Refinement of Human PSC-Derived Kidney Organoid Differentiation with Single-Cell Transcriptomics. Cell Stem Cell *23*, 869-881 e868.
Wu, Z., and McGoogan, J.M. (2020). Characteristics of and Important Lessons From the Coronavirus Disease 2019 (COVID-19) Outbreak in China: Summary of a Report of 72314 Cases From the Chinese Center for Disease Control and Prevention. JAMA.
Yang, X., Yu, Y., Xu, J., Shu, H., Xia, J.a., Liu, H., Wu, Y., Zhang, L., Yu, Z., Fang, M., *et al.* (2020). Clinical course and outcomes of critically ill patients with SARS-CoV-2 pneumonia in Wuhan, China: a single-centered, retrospective, observational study. The Lancet Respiratory Medicine.
Yang, X.H., Deng, W., Tong, Z., Liu, Y.X., Zhang, L.F., Zhu, H., Gao, H., Huang, L., Liu, Y.L., Ma, C.M., *et al.* (2007). Mice transgenic for human angiotensin-converting enzyme 2 provide a model for SARS coronavirus infection. Comp Med *57*, 450-459.
Yeung, M.L., Yao, Y., Jia, L., Chan, J.F., Chan, K.H., Cheung, K.F., Chen, H., Poon, V.K., Tsang, A.K., To, K.K., *et al.* (2016). MERS coronavirus induces apoptosis in kidney and lung by upregulating Smad7 and FGF2. Nat Microbiol *1*, 16004.
Young, B.E., Ong, S.W.X., Kalimuddin, S., Low, J.G., Tan, S.Y., Loh, J., Ng, O.-T., Marimuthu, K., Ang, L.W., Mak, T.M., *et al.* (2020). Epidemiologic Features and Clinical Course of Patients Infected With SARS-CoV-2 in Singapore. JAMA.
Zhang, F., Yang, D., Li, J., Gao, P., Chen, T., Cheng, Z., Cheng, K., Fang, Q., Pan, W., Yi, C., *et al.* (2020a). Myocardial injury is associated with in-hospital mortality of confirmed or suspected COVID-19 in Wuhan, China: A single center retrospective cohort study. medRxiv, 2020.2003.2021.20040121.
Zhang, H., Penninger, J.M., Li, Y., Zhong, N., and Slutsky, A.S. (2020b). Angiotensin-converting enzyme 2 (ACE2) as a SARS-CoV-2 receptor: molecular mechanisms and potential therapeutic target. Intensive Care Med.
Zhao, Y., Zhao, Z., Wang, Y., Zhou, Y., Ma, Y., and Zuo, W. (2020). Single-cell RNA expression profiling of ACE2, the putative receptor of Wuhan 2019-nCov. bioRxiv, 2020.2001.2026.919985.
Zhou, F., Yu, T., Du, R., Fan, G., Liu, Y., Liu, Z., Xiang, J., Wang, Y., Song, B., Gu, X., *et al.* (2020a). Clinical course and risk factors for mortality of adult inpatients with COVID-19 in Wuhan, China: a retrospective cohort study. Lancet.
Zhou, P., Yang, X.L., Wang, X.G., Hu, B., Zhang, L., Zhang, W., Si, H.R., Zhu, Y., Li, B., Huang, C.L., *et al.* (2020b). A pneumonia outbreak associated with a new coronavirus of probable bat origin. Nature.

Zhu, N., Zhang, D., Wang, W., Li, X., Yang, B., Song, J., Zhao, X., Huang, B., Shi, W., Lu, R., *et al.* (2020). A Novel Coronavirus from Patients with Pneumonia in China, 2019. N Engl J Med *382*, 727-733.

Figure1

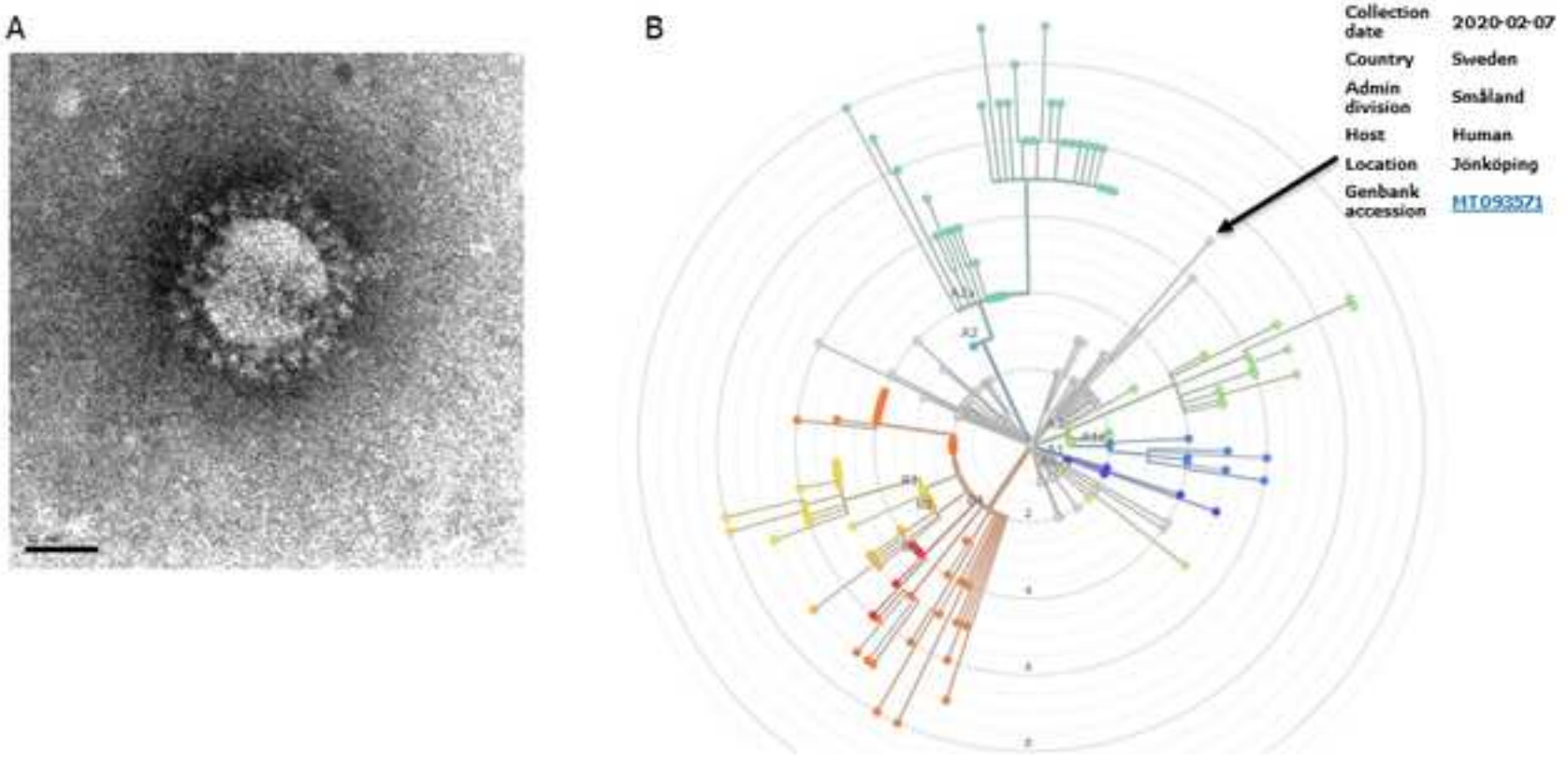
A
B
Collection date
2020-02-07
Country
Sweden
Admin division
Småland
Host
Human
Location
Jönköping
Genbank accession
MT093571

Figure2

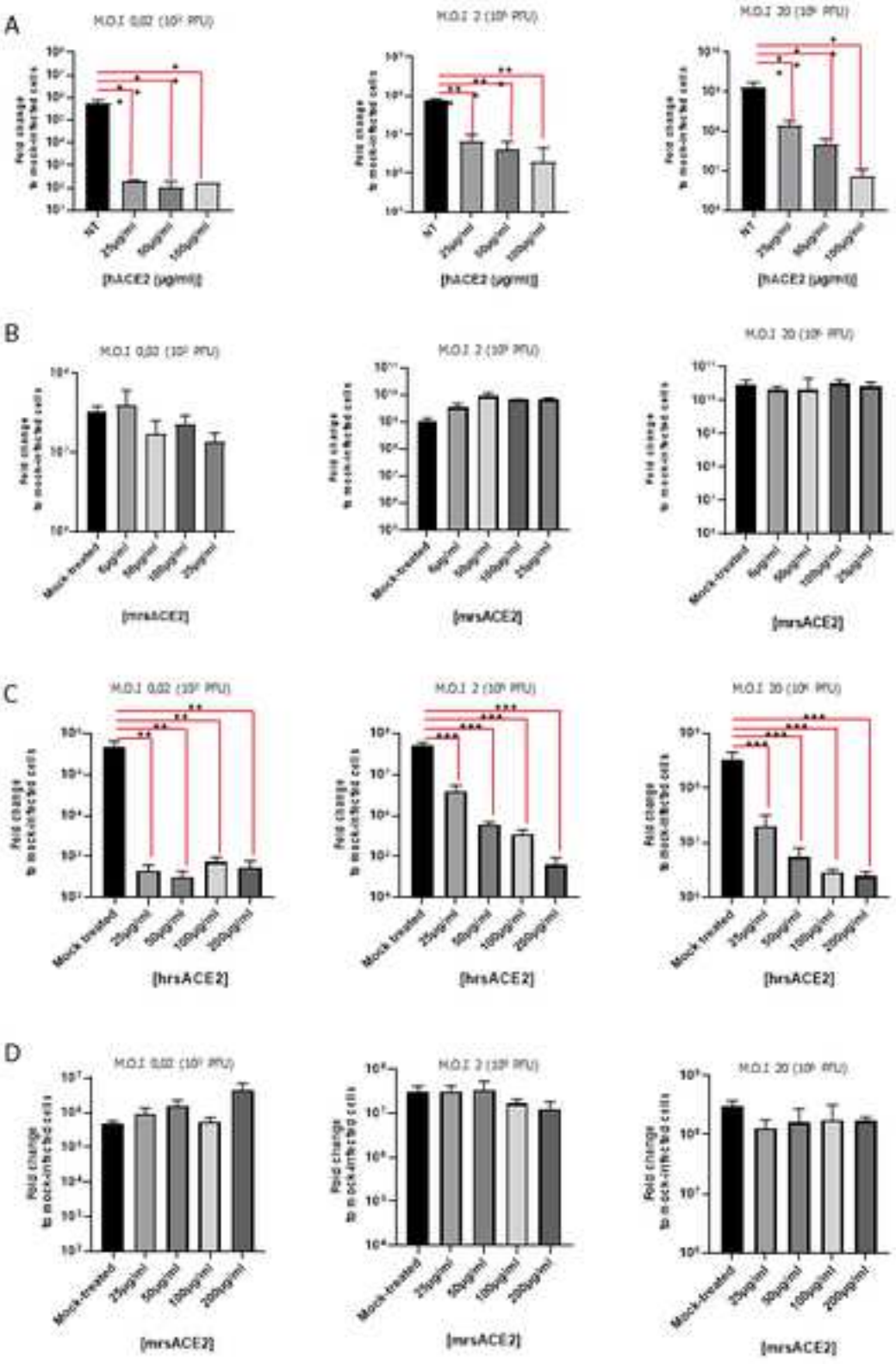
A
M.O.I 0,02 (10⁵ PFU)
M.O.I 2 (10⁵ PFU)
M.O.I 20 (10⁵ PFU)
Fold change to mock-infected cells
NT
25µg/ml
50µg/ml
100µg/ml
[hACE2 (µg/ml)]
B
M.O.I 0,02 (10⁵ PFU)
M.O.I 2 (10⁵ PFU)
M.O.I 20 (10⁵ PFU)
Fold change to mock-infected cells
Mock-treated
5µg/ml
25µg/ml
50µg/ml
100µg/ml
[mrsACE2]
C
M.O.I 0,02 (10⁵ PFU)
M.O.I 2 (10⁵ PFU)
M.O.I 20 (10⁵ PFU)
Fold change to mock-infected cells
Mock-treated
25µg/ml
50µg/ml
100µg/ml
200µg/ml
[hrsACE2]
D
M.O.I 0,02 (10⁵ PFU)
M.O.I 2 (10⁵ PFU)
M.O.I 20 (10⁵ PFU)
Fold change to mock-infected cells
Mock-treated
25µg/ml
50µg/ml
100µg/ml
200µg/ml
[mrsACE2]

Figure3

Click here to access/download;Figure;Figure 3.TIF

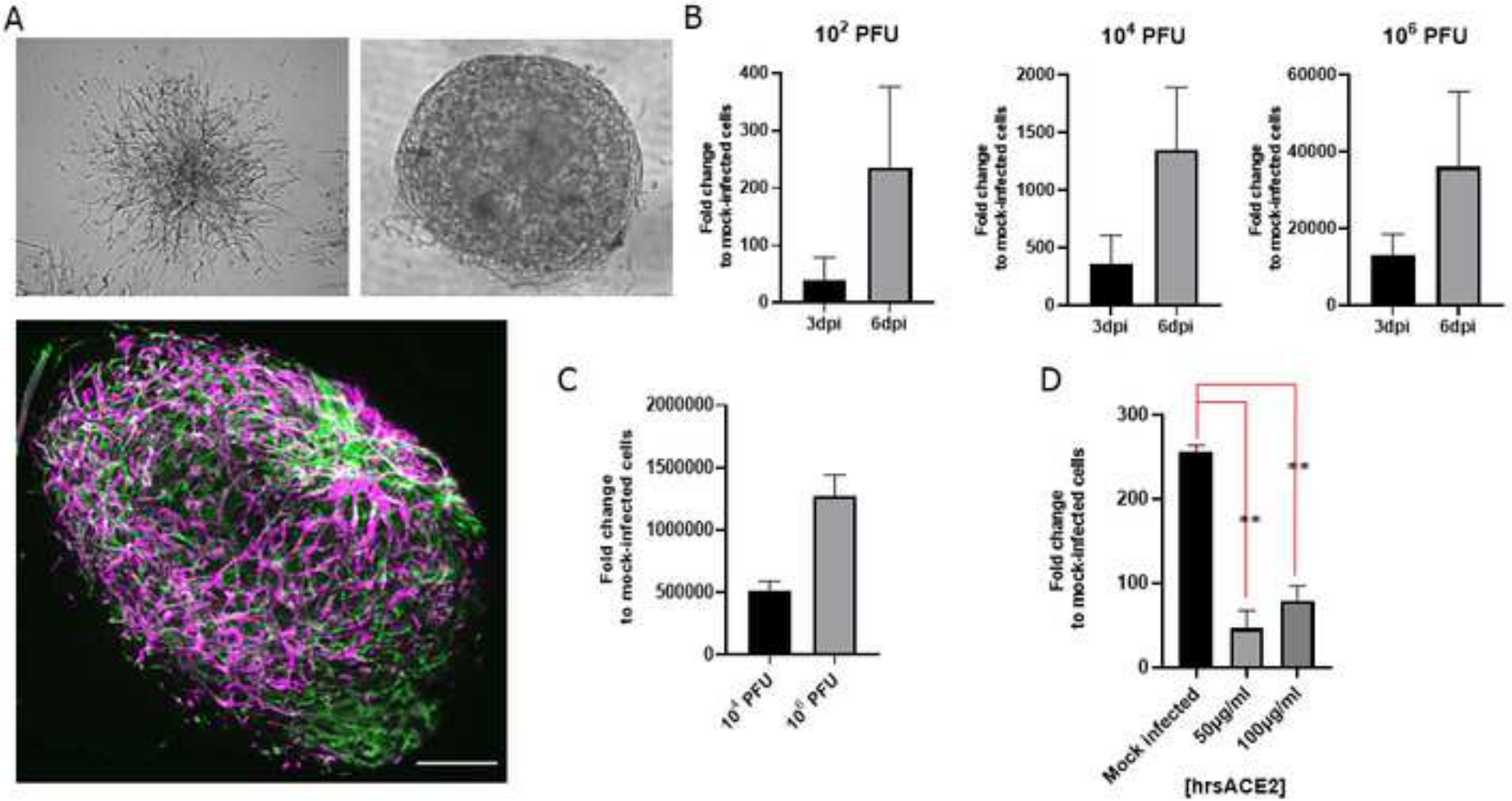

Figure4

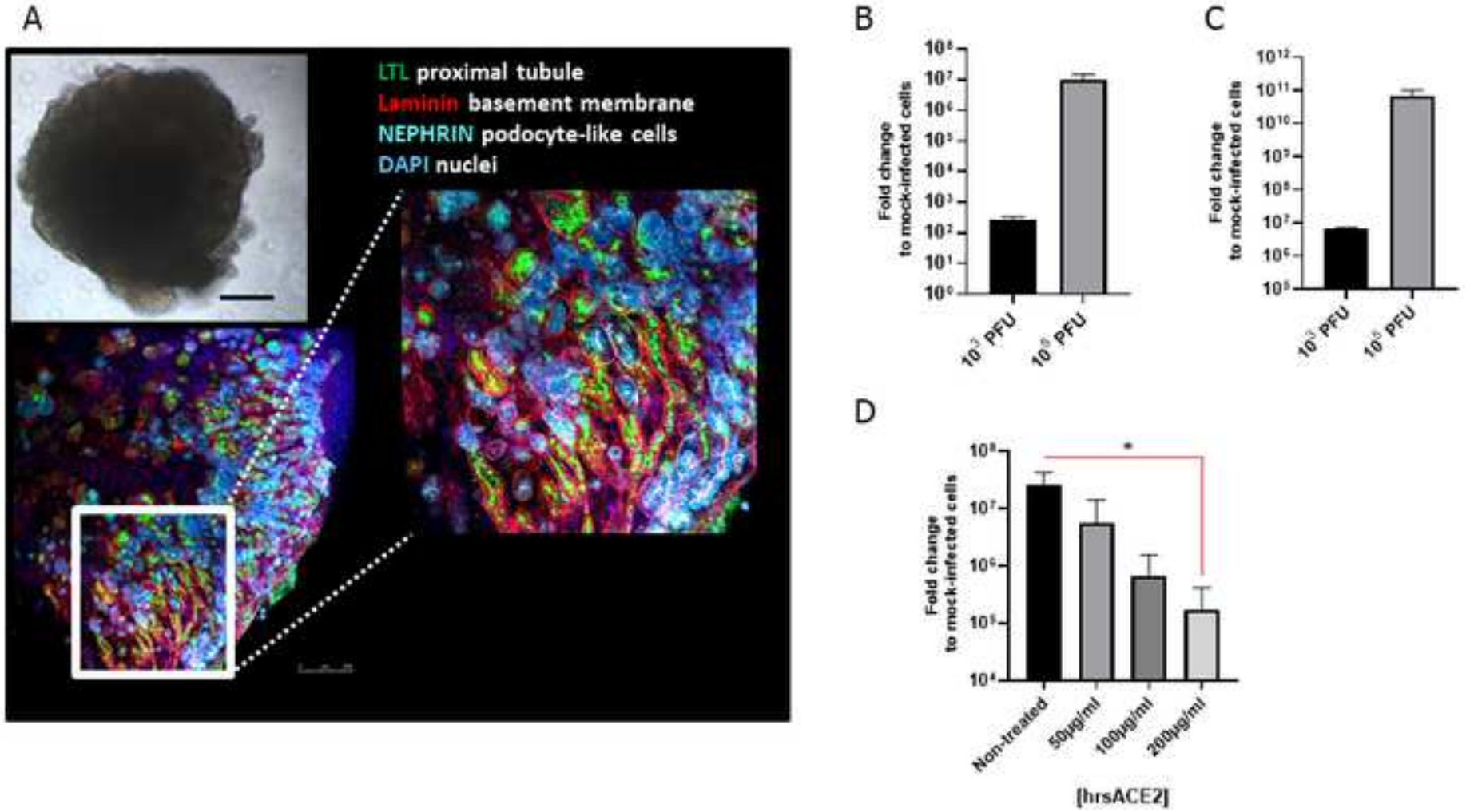
A
LTL proximal tubule
Laminin basement membrane
NEPHRIN podocyte-like cells
DAPI nuclei
B
Fold change to mock-infected cells
10³ PFU
10⁵ PFU
C
Fold change to mock-infected cells
10³ PFU
10⁵ PFU
D
Fold change to mock-infected cells
*
Non-treated
50μg/ml
100μg/ml
200μg/ml
[hrsACE2]

Supplemental Figure 1

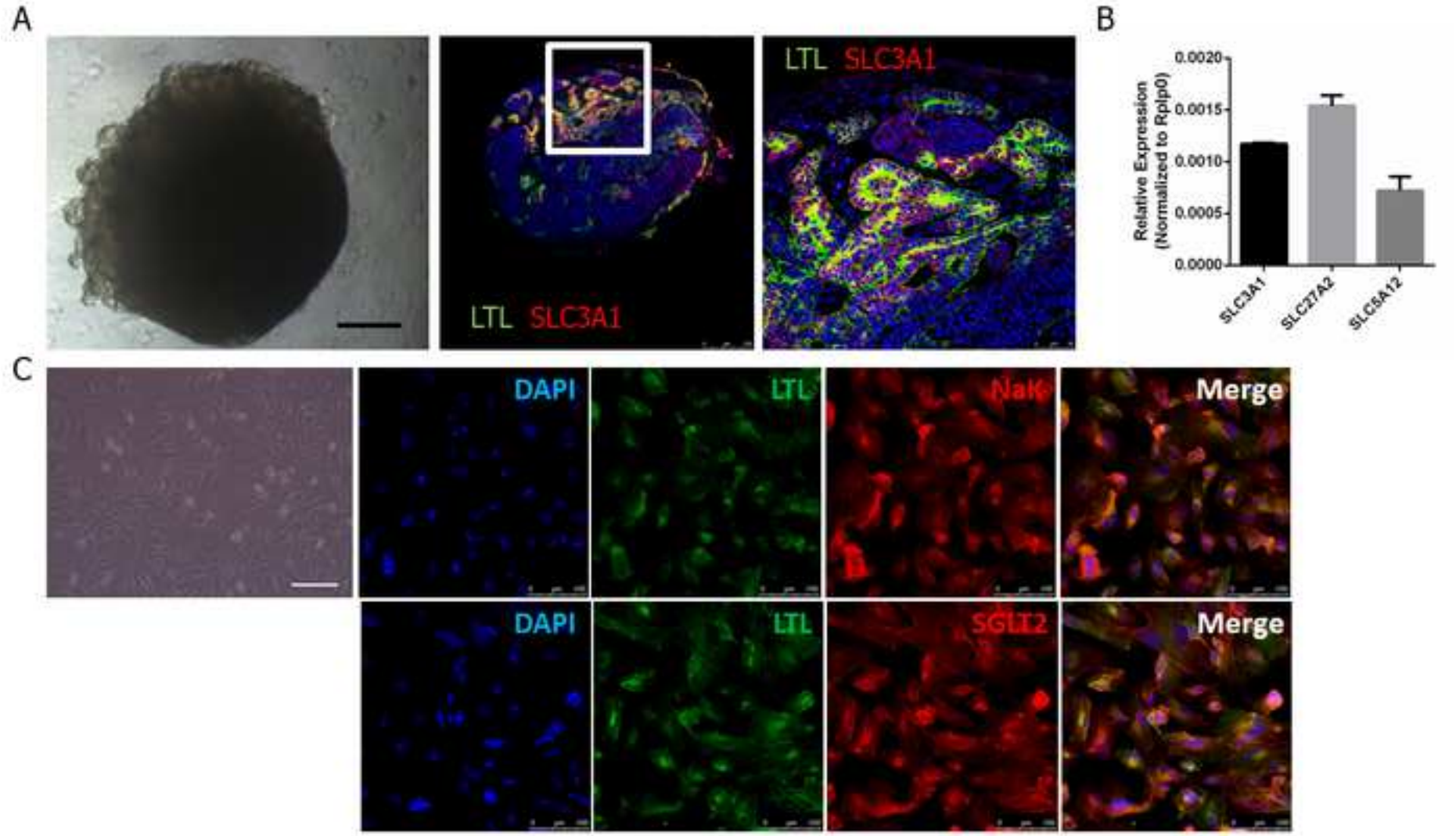

Supplemental Figure2